

Communication

A New Set of Cr_{eq} and Ni_{eq} Equations for Predicting Solidification Modes of Cast Austenitic Fe-Mn-Si-Cr-Ni Shape Memory Alloys

HUABEI PENG, YUHUA WEN, YANGYANG DU, JIE CHEN, and QIN YANG

Solidification microstructures and solidification modes in different austenitic Fe-Mn-Si-Cr-Ni shape memory alloys were investigated. Based on these results, a new set of Cr_{eq} and Ni_{eq} equations ($Cr_{eq} = Cr + 1.5Si$; $Ni_{eq} = Ni + 0.164Mn + 22C$) were developed. The above results show that Mn is still an austenite former in austenitic Fe-Mn-Si-Cr-Ni alloys containing above 12 wt pct Mn and 4 wt pct Si, but its effect is weaker than that in austenitic stainless steels with lower Mn content.

DOI: 10.1007/s11663-013-0005-8

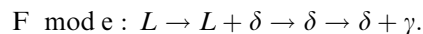
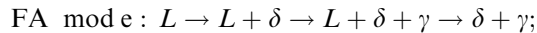
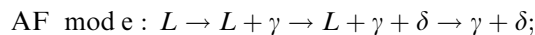
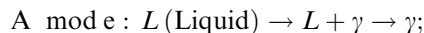
© The Minerals, Metals & Materials Society and ASM International 2013

Shape memory alloys (SMAs) have attracted attention owing to their shape memory effect (SME) and superelasticity. Fe-Mn-Si-based SMAs exhibit lower cost, better workability, and weldability as compared with Ni-Ti-based and Cu-based SMAs. Thus, there have been many studies on Fe-Mn-Si-based SMAs since Sato and his co-workers discovered the SME behavior in Fe-Mn-Si single crystals.^[1-14] Unfortunately, the recovery strain is only 2 to 3 pct in polycrystalline Fe-Mn-Si-based SMAs prepared by conventional processing techniques.^[3-14] To improve the recovery strain, the processed Fe-Mn-Si-based SMAs have to be subjected to training,^[4-6] thermo-mechanical treatment,^[9-11] or ausforming.^[8] However, the training is not only too complicated to be performed for components with complicated shapes, but also increases the production cost. The thermo-mechanical treatment and ausforming are essentially a training step. As a result, the processed Fe-Mn-Si-based SMAs have not been used commercially so far. Current research focuses mainly on developing training-free Fe-Mn-Si-based SMAs.

Very recently, Wen *et al.*^[12] developed a novel training-free cast Fe-18Mn-5.5Si-9.5Cr-4Ni alloy which solidifies primarily as delta ferrite. Its recovery strain reaches 6.4 pct,

which is higher than that of the trained Fe-14Mn-5Si-8Cr-4Ni alloy.^[13] Manufacture of parts with this alloy system is simple and less costly compared to Fe-Mn-Si-based alloy systems which require the training. Moreover, it is easy to cast components with complicated shapes. Therefore, this alloy system provides a novel way for producing a training-free Fe-Mn-Si-based alloy with the high recovery strain. In addition, it can be expected that an even higher recovery strain can be developed in cast Fe-Mn-Si-Cr-Ni SMAs through optimization of alloy compositions, casting parameters, and heat treatment techniques.

Fe-Mn-Si-Cr-Ni SMAs are a special kind of austenitic stainless steels. There exist four types of solidification mode in austenitic stainless steels, *i.e.*, austenitic (A), austenitic-ferritic (AF), ferritic-austenitic (FA), and ferritic (F) modes. The four solidification modes are determined according to solidification sequence, as follows.^[15,16]



Different solidification modes produce distinctive as-cast microstructures, inevitably leading to different SME behaviors. Obviously, it is of importance to investigate the effect of solidification modes on solidification microstructures and their resulting SME. However, our previous work showed that four sets of Cr_{eq} and Ni_{eq} equations (Delong *et al.*^[17] Hull,^[18] Hammar and Svensson^[19,20] as well as WRC-1992^[21] equations) and Thermo-Calc software[®] are invalid to predict the solidification modes of cast Fe-(13-27)Mn-5.5Si-8.5Cr-5Ni SMAs.^[22] Therefore, a new set of Cr_{eq} and Ni_{eq} equations has to be developed to predict the solidification modes of cast Fe-Mn-Si-Cr-Ni SMAs. In the present paper, we investigated solidification microstructures of cast Fe-(13-27)Mn-(4.5-6.5)Si-(7-9)Cr-(4-6)Ni SMAs and determined their solidification modes according to their microstructural features. Based on their solidification modes, a new set of Cr_{eq} and Ni_{eq} equations was successfully developed.

Cast Fe-Mn-Si-Cr-Ni SMAs were prepared by the method described in Reference^[22]. Chemical compositions of the cast Fe-Mn-Si-Cr-Ni SMAs are listed in Table I. Solidification modes were determined using optical metallography. F mode was determined by ordinary optical micrographs etched using 1 g $C_2H_2O_4$ + 15 mL H_2O_2 + 1 mL HF + 15 mL distilled water (referred as Etchant 1). FA, AF, and A modes were determined by a color metallographic technique developed by Rajasekhar *et al.*^[16] The etchant is 0.5 g $K_2S_2O_5$ + 20.0 g NH_4HF_2 + 100 mL distilled water (referred as Etchant 2). The skeletal structure presenting in dendritic centers represents the FA mode, while the mixture of cellular and dendritic structure

HUABEI PENG, Lecturer, YUHUA WEN, Professor, YANGYANG DU, JIE CHEN, and QIN YANG, Postgraduates, are with the College of Manufacturing Science and Engineering, Sichuan University, Chengdu 610065, People's Republic of China. Contact e-mail: wenyh-mse@126.com

Manuscript submitted July 15, 2013.

Article published online December 3, 2013.

Table I. Chemical Compositions and Solidification Modes of Cast Fe-Mn-Si-Cr-Ni SMAs

Cast Alloys	Chemical Compositions (wt pct)						Solidification Modes
	Si	Cr	Mn	Ni	C	Fe	
13Mn	5.83	9.06	12.50	4.87	0.012	bal.	F
15Mn	5.78	8.85	14.72	4.76	0.013	bal.	F
17Mn	5.45	7.37	16.42	5.07	0.008	bal.	F
19Mn	5.70	8.91	18.54	4.45	0.008	bal.	F
21Mn	5.65	8.95	20.98	4.72	0.006	bal.	F
23Mn	5.62	8.97	22.82	5.03	0.007	bal.	F/FA
25Mn	5.89	8.91	24.43	5.00	0.007	bal.	FA
27Mn	5.63	8.84	26.15	5.41	0.008	bal.	FA
4.5Si	4.44	9.08	18.42	5.06	0.008	bal.	FA
6.5Si	6.24	8.94	19.71	4.93	0.009	bal.	F
4Ni	5.35	8.98	19.69	4.04	0.008	bal.	F
5Ni	5.73	9.10	19.64	5.12	0.008	bal.	F
6Ni	5.47	8.64	20.51	5.92	0.009	bal.	FA

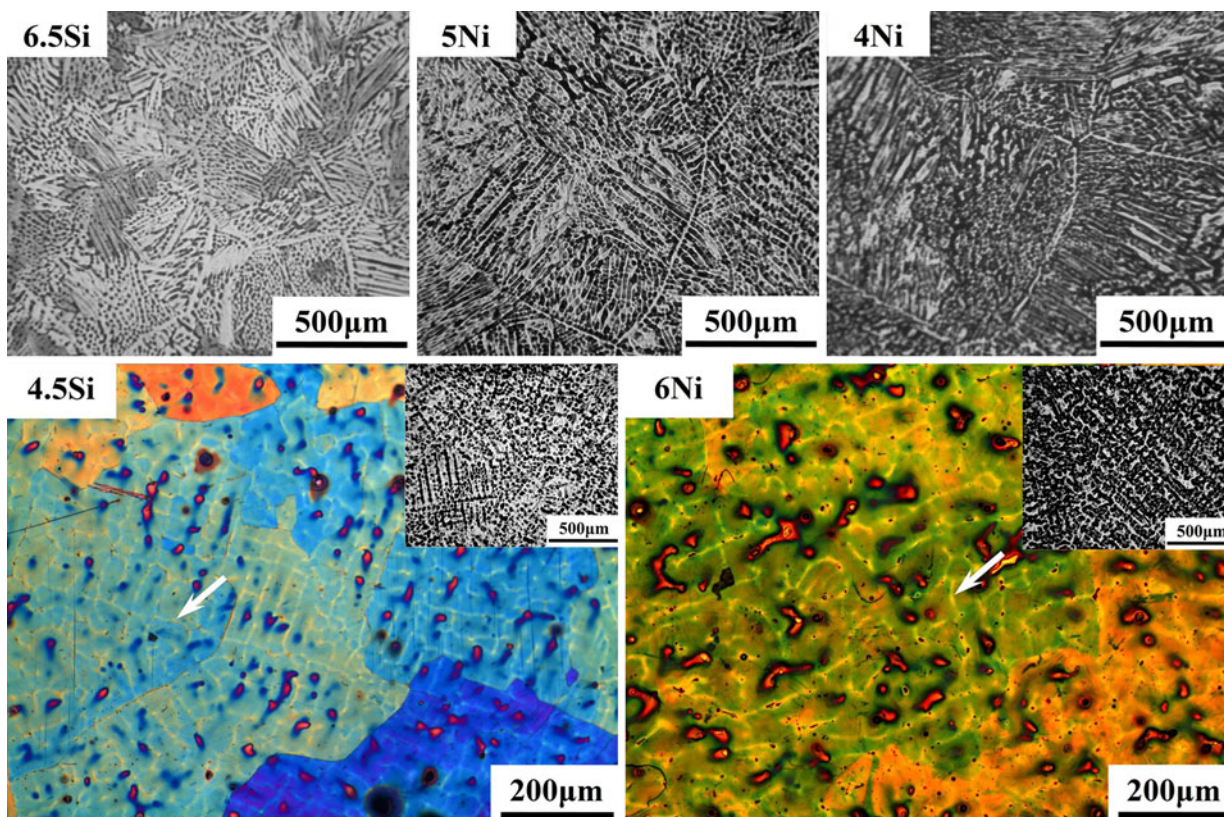


Fig. 1—Optical micrographs of cast Fe-Mn-Si-Cr-Ni alloys. Ordinary optical micrographs etched by Etchant 1, color optical micrographs etched by Etchant 2.

represents the AF mode. The dendritic structure represents the A mode. For cast 13Mn-27Mn alloys listed in Table I, we have determined their solidification modes in our previous work.^[22] In the present paper, we investigated solidification microstructures of other cast Fe-Mn-Si-Cr-Ni alloys listed in Table I, as illustrated in Figure 1. In the ordinary optical micrographs, the microstructures of 6.5Si, 4Ni, and 5Ni alloys are the typical Widmanstätten morphology, whereas the microstructures of 4.5Si and 6Ni alloys are the dendritic morphology. F mode results in the Widmanstätten

microstructure.^[15,16] Therefore, the solidification mode of 6.5Si, 4Ni, and 5Ni alloys is the F mode. However, we cannot determine the solidification mode of 4.5Si and 6Ni alloys only according to their dendritic morphology. In order to determine their solidification modes, we used the color metallographic technique. The results showed that in the color micrographs, the skeletal structure (indicated by white arrows) presents in the dendritic centers of 4.5Si and 6Ni alloys, indicating that their solidification mode is the FA mode. In the research completed so far, only F and FA modes of cast Fe-Mn-

Table II. Four Sets of Cr_{eq} and Ni_{eq} Equations Predicting Solidification Modes of Austenitic Stainless Steels

Names of Equation	Cr _{eq} =	Ni _{eq} =
Delong <i>et al.</i> ^[17]	Cr + 1.5Si + Mo + 0.5Nb	Ni + 0.5Mn + 30C + 30N
Hull ^[18]	Cr + 0.48Si + 0.14Nb + 2.2Ti	Ni + 0.11Mn - 0.0086Mn ² + 24.5C + 18.4N + 0.44Cu
Hammar and Svensson ^[20]	Cr + 1.5Si + 1.37Mo + 2Nb + 3Ti	Ni + 0.31Mn + 22C + 14.2N + Cu
WRC-1992 ^[21]	Cr + Mo + 0.7Nb	Ni + 35C + 20N + 0.25Cu

Hammar and Svensson equation, A: Cr_{eq}/Ni_{eq} < 1.35; AF: 1.35 < Cr_{eq}/Ni_{eq} < 1.50; FA 1.50 < Cr_{eq}/Ni_{eq} < 1.95; F: Cr_{eq}/Ni_{eq} < 1.95^[20]

Table III. Predicted Solidification Modes of Cast Fe-Mn-Si-Cr-Ni SMAs by New Two Sets of Cr_{eq} and Ni_{eq} Equations

Cast Alloys	Actual Solidification Modes	First Set of Cr _{eq} and Ni _{eq} Equations		Second Set of Cr _{eq} and Ni _{eq} Equations	
		Cr _{eq} /Ni _{eq}	Predicted Solidification Modes	Cr _{eq} /Ni _{eq}	Predicted Solidification Modes
13Mn	F	2.48	F	2.73	F
15Mn	F	2.35	F	2.52	F
17Mn	F	1.96	F	2.12	F
19Mn	F	2.28	F	2.32	F
21Mn	F	2.10	F	2.11	F
23Mn	F/FA	1.95	F/FA	1.95	F/FA
25Mn	FA	1.94	FA	1.93	FA
27Mn	FA	1.75	FA	1.74	FA
4.5Si	FA	1.91	FA	1.91	FA
6.5Si	F	2.19	F	2.27	F
4Ni	F	2.28	F	2.24	F
5Ni	F	2.08	F	2.14	F
6Ni	FA	1.78	FA	1.86	FA

Si-Cr-Ni SMAs were attained through adjusting the chemical compositions, as seen in Table I.

For the purpose of developing a new set of Cr_{eq} and Ni_{eq} equations to predict the solidification modes of cast Fe-Mn-Si-Cr-Ni SMAs, the first step was to analyze why four sets of Cr_{eq} and Ni_{eq} equations (Table II) are invalid to predict their solidification modes. The WRC-1992 equation does not consider the influence of Mn and Si on the solidification behavior. Therefore, it cannot predict the solidification modes of cast Fe-Mn-Si-Cr-Ni SMAs. In the case of the Hull equation, Mn suppressed the formation of austenite when it was above about 12.79 wt pct. However, our previous work showed that Mn still promotes the formation of austenite when it is above 12 wt pct.^[22] The Delong *et al.* equation^[17] is derived from welding studies, and the equation attributed to Hammar and Svensson^[19] was derived from studies of small samples by thermal analysis. Generally, the cooling rate of our cast Fe-Mn-Si-Cr-Ni SMAs is between 0.6 and 60 K/min,^[23] and is much lower than that of weld metals which typically cool at a rate of 4000 K/min,^[24] and is a magnitude similar to that of thermal analysis experiments conducted by Hammar and Svensson, which was typically 20 K/min.^[19] However, the Hammar and Svensson equation does not correctly predict the solidification modes of cast Fe-Mn-Si-Cr-Ni SMAs.^[22] Note that the Mn and Si concentrations are above 12 and 4 wt pct, respectively, in the cast Fe-Mn-Si-Cr-Ni alloys while are below 2 and 0.8 wt pct, respectively, in the thermal analysis samples investigated by Hammar and Svensson. Furthermore, the Cr and Ni

concentrations in the thermal analysis samples are much higher than that in the cast Fe-Mn-Si-Cr-Ni alloys. Accordingly, the coefficient of Mn or Si in the Hammar and Svensson equation is unsuitable for predicting the solidification modes of cast Fe-Mn-Si-Cr-Ni alloys because the Cr, Ni, Mn, and Si concentrations in the cast Fe-Mn-Si-Cr-Ni alloys is much different from that in the thermal analysis samples. Based on the above analysis, a new set of Cr_{eq} and Ni_{eq} equations would be developed through revising the coefficient of Mn or Si in the Hammar and Svensson equation.

Our previous study showed that the solidification mode of 23Mn alloy is a mixture of F and FA modes (Table I).^[22] Therefore, the Cr_{eq}/Ni_{eq} value of 23Mn alloy is approximately the critical value, over which the solidification mode changes from F to FA mode. In the case of Hammar and Svensson equation, this critical Cr_{eq}/Ni_{eq} value is 1.95.^[20] Thus, when we only corrected the coefficient of Mn element in Hammar and Svensson equation, a revised coefficient for Mn was calculated to be a value of 0.164, from the following Eq. [1].

$$\begin{aligned} \frac{Cr_{eq}}{Ni_{eq}} &= \frac{1 \times Cr + 1.5 \times Si}{1 \times Ni + (\text{Coefficient of Mn}) \times Mn + 22 \times C} \\ &= \frac{1 \times 8.97 + 1.5 \times 5.62}{1 \times 5.03 + (\text{Coefficient of Mn}) \times 22.82 + 22 \times 0.007} \\ &= 1.95 \end{aligned} \quad [1]$$

The first new set of Cr_{eq} and Ni_{eq} equations was developed as follows:

Table IV. Designed Chemical Compositions and Predicted Solidification Modes of Two Cast Fe-Mn-Si-Cr-Ni SMAs by New Two Sets of Cr_{eq} and Ni_{eq} Equations

Cast Alloys	Designed Chemical Compositions (wt pct)						First Set of Cr_{eq} and Ni_{eq} Equations		Second Set of Cr_{eq} and Ni_{eq} Equations	
	Si	Cr	Mn	Ni	C	Fe	Cr_{eq}/Ni_{eq}	Predicted Solidification Modes	Cr_{eq}/Ni_{eq}	Predicted Solidification Modes
#1	5.5	6.0	21.0	8.5	–	bal.	1.19	A	1.37	AF
#2	5.5	6.5	21.0	6.5	–	bal.	1.48	AF	1.62	FA

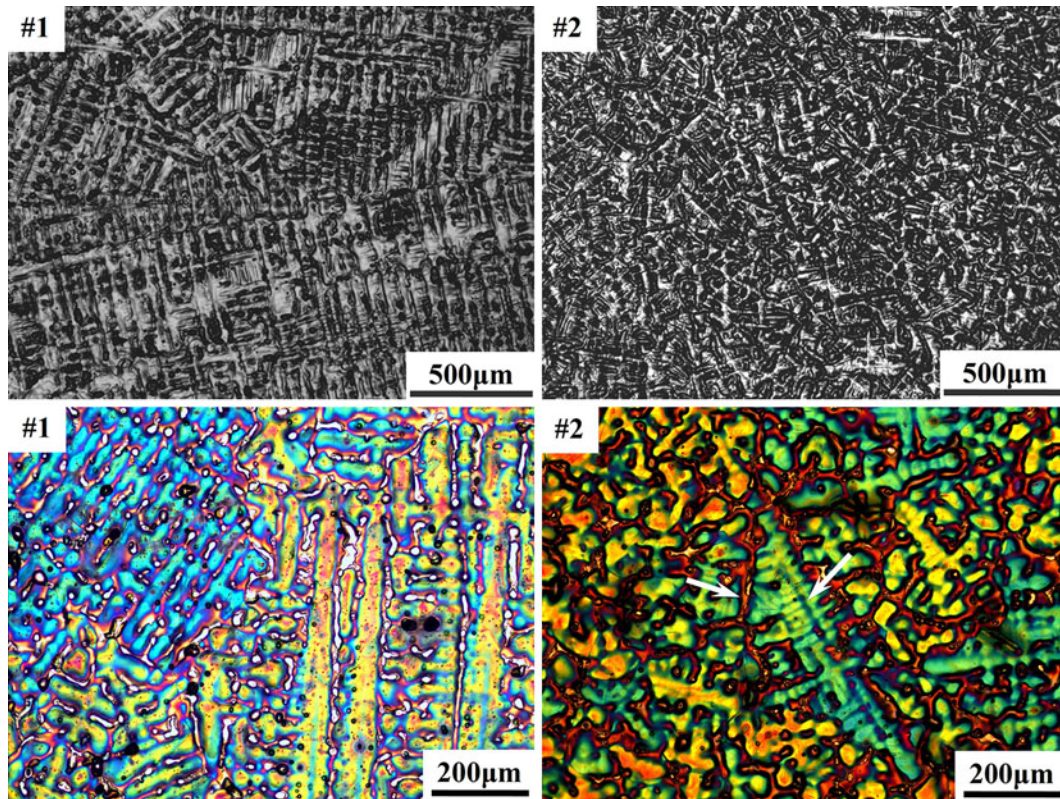


Fig. 2—Optical micrographs of cast Alloys #1 and #2. Ordinary optical micrographs etched by Etchant 1, color optical micrographs etched by Etchant 2.

$$Cr_{eq} = Cr + 1.5Si; \quad Ni_{eq} = Ni + 0.164Mn + 22C.$$

Similarly, when we only corrected the coefficient of Si element in Hammar and Svensson equation, a revised coefficient for Si was calculated to be a value of 2.66, from the following Eq. [2].

$$\frac{Cr_{eq}}{Ni_{eq}} = \frac{1 \times Cr + (\text{Coefficient of Mn}) \times Si}{1 \times Ni + 0.31 \times Mn + 22 \times C} \quad [2]$$

$$= \frac{1 \times 8.97 + (\text{Coefficient of Si}) \times 5.62}{1 \times 5.03 + 0.31 \times 22.82 + 22 \times 0.007} = 1.95$$

The second new set of Cr_{eq} and Ni_{eq} equations was developed as follows:

$$Cr_{eq} = Cr + 2.66Si; \quad Ni_{eq} = Ni + 0.31Mn + 22C.$$

For new two sets of Cr_{eq} and Ni_{eq} equations, A, AF, FA, and F modes correspond to the following range of Cr_{eq}/Ni_{eq} value, which is same as the Hammar and Svensson equation:^[20] A: $Cr_{eq}/Ni_{eq} < 1.35$; AF: $1.35 < Cr_{eq}/Ni_{eq} < 1.50$; FA: $1.50 < Cr_{eq}/Ni_{eq} < 1.95$; F: $Cr_{eq}/Ni_{eq} > 1.95$.

Based on new two sets of Cr_{eq} and Ni_{eq} equations, Table III lists the predicted solidification modes of cast Fe-(13–27)Mn-(4.5–6.5)Si-(7–9)Cr-(4–6)Ni SMAs. The results showed that both are valid to predict the F and FA modes of cast Fe-Mn-Si-Cr-Ni SMAs. To further examine whether the two sets of Cr_{eq} and Ni_{eq} equations can predict the A and AF modes of cast Fe-Mn-Si-Cr-Ni SMAs, we designed two cast Fe-Mn-Si-Cr-Ni SMAs. The solidification modes of Alloys #1 and #2 are A and AF, respectively, according to the first new set of Cr_{eq} and Ni_{eq} equations while they are AF and FA, respec-

Table V. Actual Chemical Compositions as Well as Predicted and Actual Solidification Modes of Two Cast Fe-Mn-Si-Cr-Ni SMAs

Cast Alloys	Actual Chemical Compositions (wt pct)						First Set of Cr_{eq} and Ni_{eq} Equations		Second Set of Cr_{eq} and Ni_{eq} Equations		Actual Solidification Modes
	Si	Cr	Mn	Ni	C	Fe	Cr_{eq}/Ni_{eq}	Predicted Solidification Modes	Cr_{eq}/Ni_{eq}	Predicted Solidification Modes	
#1	5.33	5.48	21.20	8.81	0.020	bal.	1.06	A	1.24	A	A
#2	5.52	6.92	21.24	6.85	0.007	bal.	1.45	AF	1.59	FA	AF

tively, according to the second new set of Cr_{eq} and Ni_{eq} equations (Table IV). Figure 2 shows ordinary and color optical micrographs of Alloys #1 and #2. In the ordinary optical micrographs, the microstructures of Alloys #1 and #2 are the dendritic morphology. Moreover, the dendritic structure of Alloy #1 is coarser than that of Alloy #2. In the color micrographs, the microstructure of Alloy #1 is also the dendritic morphology, but the microstructure of Alloy #2 is a mixture of cellular and dendritic morphology (indicated by white arrows). Accordingly, the solidification mode of Alloy #1 is the A mode, and that of Alloy #2 the AF mode. Table V gives the actual chemical compositions as well as the predicted and actual solidification modes of the two cast Fe-Mn-Si-Cr-Ni SMAs. This result shows that the first new set of Cr_{eq} and Ni_{eq} equations ($Cr_{eq} = Cr + 1.5Si$; $Ni_{eq} = Ni + 0.164Mn + 22C$) is able to predict the A and AF modes of the two cast Fe-Mn-Si-Cr-Ni SMAs, while the second new set of Cr_{eq} and Ni_{eq} equations ($Cr_{eq} = Cr + 2.66Si$; $Ni_{eq} = Ni + 0.31Mn + 22C$) does not correctly predict the solidification modes.

In Cr_{eq} and Ni_{eq} equations, the coefficients associated with each element represent their ability to promote the formation of austenite or ferrite. The larger the coefficients of elements, the stronger their effect. The coefficient for Mn is 0.31 in the Hammar and Svensson equation,^[20] but it reduces to 0.164 in our new set of Cr_{eq} and Ni_{eq} equations. Note that the Hammar and Svensson equation was derived from the thermal analysis samples whose Mn concentrations were below 2 wt pct, while our new set of Cr_{eq} and Ni_{eq} equations was derived from the cast Fe-Mn-Si-Cr-Ni alloys whose Mn concentrations were 12 to 27 wt pct. Accordingly, the effect of Mn promoting the formation of austenite is much stronger when its concentration is below 2 wt pct than when its concentration is 12 to 27 wt pct. This result indicates that the effect of Mn is nonlinear, and thus the coefficient of Mn in Ni_{eq} equation is not a constant. This is the reason why Hammar and Svensson equation does not correctly predict the solidification modes of cast Fe-Mn-Si-Cr-Ni SMAs.

In summary, the solidification microstructures in different Fe-Mn-Si-Cr-Ni SMAs had been studied. According to their distinctive solidification microstructures, their solidification modes were determined. Based on these results, we developed a new set of Cr_{eq} and Ni_{eq} equations ($Cr_{eq} = Cr + 1.5Si$; $Ni_{eq} = Ni + 0.164Mn + 22C$). This set of Cr_{eq} and Ni_{eq} equations can predict the solidification modes of cast Fe-Mn-Si-Cr-Ni

SMAs. The above results show that Mn is still an austenite former. However, its effect is nonlinear and is weaker in Fe-Mn-Si-Cr-Ni SMAs containing above 12 wt pct Mn and 4 wt pct Si than in austenitic stainless steels with lower Mn concentration. The new set of Cr_{eq} and Ni_{eq} equations will lay the foundation for designing cast Fe-Mn-Si-Cr-Ni alloys with different solidification modes, investigating the effects of solidification modes on the as-cast microstructure and SME.

The work was supported by the National Natural Science Foundation of China (Nos. 50871072, 50971095, and 51171123), the Natural Science Foundation for Young Scientists of Sichuan Province in China (No. 2010A01-436), and the Fundamental Research Funds for the Central Universities (No. 2012SCU11068).

REFERENCES

1. A. Sato, E. Chishima, K. Soma, and T. Mori: *Acta Metall. Mater.*, 1982, vol. 30, pp. 1177–83.
2. A. Sato, Y. Yamaji, and T. Mori: *Acta Metall.*, 1985, vol. 34, pp. 287–94.
3. H. Otsuka, H. Yamada, T. Maruyama, T. Mori, H. Tanahashi, S. Matsuda, and M. Murakami: *ISIJ Int.*, 1990, vol. 30, pp. 674–79.
4. Y. Watanabe, Y. Mori, and A. Sato: *J. Mater. Sci.*, 1993, vol. 28, pp. 1509–14.
5. Q. Gu, J.V. Humbeeck, and L. Delaey: *J. Phys. VI*, 1994, vol. 4, pp. 135–44.
6. S. Kajiwaru: *Mater. Sci. Eng. A*, 1999, vols. 273–275, pp. 67–88.
7. S. Kajiwaru, D. Liu, T. Kikuchi, and N. Shinya: *Scripta Mater.*, 2001, vol. 44, pp. 2809–14.
8. D.F. Wang, D.Z. Liu, Z.Z. Dong, W.X. Liu, and J.M. Chen: *Mater. Sci. Eng. A*, 2001, vol. 315, pp. 174–79.
9. A. Baruj, T. Kikuchi, S. Kajiwaru, and N. Shinya: *Mater. Sci. Eng. A*, 2004, vol. 378, pp. 333–36.
10. N. Stanford and D.P. Dunne: *Mater. Sci. Eng. A*, 2006, vol. 422, pp. 352–59.
11. Y.H. Wen, W. Zhang, N. Li, H.B. Peng, and L.R. Xiong: *Acta Mater.*, 2007, vol. 55, pp. 6526–34.
12. Y.H. Wen, H.B. Peng, P.P. Sun, G. Liu, and N. Li: *Scripta Mater.*, 2010, vol. 62, pp. 55–58.
13. Y.H. Wen, H.B. Peng, C.P. Wang, Q.X. Yu, and N. Li: *Adv. Eng. Mater.*, 2011, vol. 13, pp. 48–56.
14. X.H. Min, T. Sawaguchi, X. Zhang, and K. Tsuzakia: *Scripta Mater.*, 2012, vol. 67, pp. 37–40.
15. J.C. Lippold and D.J. Kotecki: *Welding Metallurgy and Weldability of Stainless Steels*, 1st ed., Wiley-Interscience, Hoboken, 2005.
16. K. Rajasekhar, C.S. Harendranath, R. Raman, and S.D. Kulkarni: *Mater. Charact.*, 1997, vol. 38, pp. 53–65.

17. W.T.C. Delong, G.A. Ostrom, and E.R. Szumachowski: *Weld. J.*, 1956, vol. 35, pp. 526–32.
18. F.C. Hull: *Weld. J.*, 1973, vol. 52, pp. 193–203.
19. Ö. Hammar and U. Svensson: in *Solidification and Casting of Metals*, Metal Society, Book 192, London, 1979, pp. 401–410.
20. *ASM Handbook, Volume 6: Welding, Brazing and Soldering*, 10th ed., ASM International, Materials Park, OH, 1993.
21. D. Kotecki and T.A. Siewert: *Weld. J.*, 1992, vol. 71, pp. 171–78.
22. H.B. Peng, Y.H. Wen, Y.Y. Du, Q.X. Yu, and Q. Yang: *Metall. Mater. Trans. B*, 2013, vol. 44B, pp. 1137–43.
23. M.C. Flemings: *Proc. F. Weinberg Int. Symp. Solidif. Process.*, 1990, pp. 173.
24. N. Suutala: *Metall. Trans. A*, 1983, vol. 14A, pp. 191–196.